

Analysis of Land Subsidence Deformation Caused by Urban Shallow-buried Tunnel Construction

Donglin Wang*, Xin Guo and Yusheng Jia

School of Civil Engineering, Anhui Jianzhu University, Hefei, Anhui, China

Abstract: Taking the project of Hefei city plaza tunnel as an example, this paper takes the large-scale finite element calculation software of ABAQUS to set three dimensional calculations models to simulate the construction of underground tunnel, analyzing the displacement and stress dynamic response during the construction process. And the paper also carries out the comparison analysis of the field measurement of the land subsidence. The result indicates that the simulation objectively reflected the rules of subsidence during the construction process. This provides theory evidence for shallow-buried tunnel construction safely and rapidly.

Keywords: Land subsidence, numerical simulation, shallow-buried tunnel.

1. INTRODUCTION

With the rapid development of city construction, aboveground space is facing more and more pressure. Seeking space from underground has become a historical trend in cities' developing path. Underground space would be exploited and utilized vigorously [1-3]. Since the underground construction will be done within the rock and soil mass. In spite of the degree of the buried depth, the excavation construction will inevitably weak the underground rock and soil mass which will result in the change that the origin broken equilibrium state would turn into new equilibrium state [4, 5]. Serious land subsidence and collapse would happen and therefore the damage of the road pavement, buildings and underground pipeline [6-8]. Now according to the reality of the Hefei city Plaza tunnel, this paper utilizes the large scale finite element ABAQUS to carry on the analysis of settlement deformation caused by shallow-buried tunnel construction under complex situations, in order to obtain experiences on design and operation for similar underground engineering.

2. PROJECT PROFILE

The whole length of Hefei city plaza tunnel is 59.5 m with 6 m net width of which 17.5 m is constructed by open cut method of frame structure design. While the other part under the Huizhou Road and the city plaza is practiced by undermining methods since the limitation of the cars and pedestrians. The length of this part is 42 m, circular arch lining of 3m buried depth. The excavation section is ellipse of 6 m net width and 2.5 m net height, in which the excavation height is 8.48 m and the excavation width 5.6 m,

as shown in Fig. (1). This part is constructed by using the combined technology of long pipe roof and small duct pregrouting construction techniques. The length of the pipe roof is 42 m and the circular spacing 0.4 m; Small duct pregrouting is $\phi 42 \times 3.5$ mm hot rolling seamless pipe. The length of the pipe is 4.1 m and the circular spacing is 0.4 m, with a 7° extrapolation angel.

2.1 Geological Situation

According to the field drilling and testing result combing with the indoor geotechnical experiments, the soil of this site can be divided from top to bottom into:

(1) Miscellaneous Fill Layer

The thickness of the layer is 3.6~5.0 m and the bottom elevation is 9.08~10.05 m. The color is of grey black and variegation. The surface is 0.3 m thick consisted of concrete and pavement. Under the surface is plain backfill, contains cinder, much gravel and little bit lime-soil and much mucky soil.

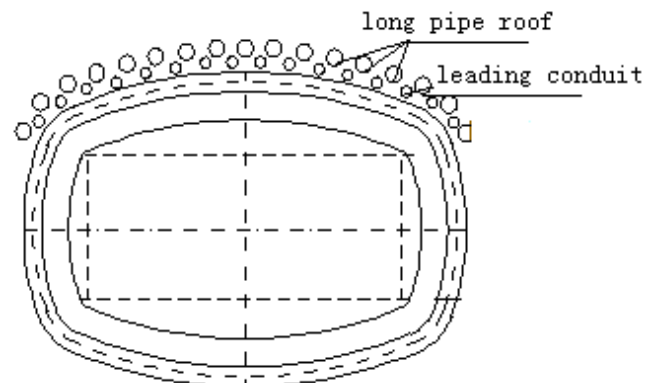


Fig. (1). Underground tunnel section.

*Address correspondence to this author at School of Civil Engineering, Anhui Jianzhu University, 292 Ziyun Road, Hefei City, Anhui Province, China.; Tel: 13695698055; E-mail: wdlvip@126.com

(2) Silt Miscellaneous Fill Layer

The thickness of this layer is 3.2~6.5 m, with the bottom elevation 2.58 m~6.58 m. The color is grey black color and the density is loose (soft-plastic-flow plastic) with high water content. This layer presents saturation status for containing stinking humus, and gravel and rotten wood.

(3) Sandy Loam interbeds of Siltstone Layer

This layer spreads obviously under the southern tunnel part of the site. The thickness is 3.8 m~3.2 m and layer bottom elevation 2.65~3.30 m of grey white color. The density of this layer is Slight to medium with high water containment which presented to be saturated. This layer contains little iron oxide and fine sand.

(4) Fine Sand and Sandy Loam interbeds Layer

This layer generally distributed under the site of 7.0 m~8.7 m thickness. The layer bottom elevation is -5.70 m~-4.42 m and the color is grey brown and grey green of medium to high density. This layer represents a saturation state. With part inclusion of silt soil thin layer, this layer contains some grey green and purple red hard particles of which the chief mineral compositions are quartz, feldspar and mica and etc.

2.2. Hydrological Situation

There are two types of ground water of this site. One is perched water which could be found at ① Miscellaneous Fill Layer and ② Mucky Miscellaneous Fill Layer. Since the fill of the two layers are thick and loose, the amount of the water is large. The main recharge of this water relies on the meteoric water, leakage of nearby rain pipe and waste water pipe. The entire underground water keeps a unified water level. The discharge forms for this type are evaporation and infiltration to the low lying.

The other groundwater is among the ③ Sandy Loam interbeds of Siltstone and Fine Sand Layer and ④ Sandy Loam Interbed Layer. The water amount is rich and mainly recharged by the rain water, surface water infiltration and underground runoff. The buried depth of the underground water static water level is 0.8~2.0 m, and the static water surface elevation is 11.7 m~12.9 m with a 2 m around water surface change amplitude.

2.3. Technology Characteristic and Difficulties

1) The geological condition is odious. The upper soil of the tunnel is miscellaneous fill, while that of 3-8 m is saturated saltation clay deposited for several years from JinDou River. The soil of 8-18 m is saturated of sandy soil of extremely poor self-stability. Roof fall and over deformation will easily occur during the construction.

2) The buried depth of the tunnel is particularly shallow that only 3 m left between the tunnel roof and the ground surface.

3) Many line pipes such as gas, electric power, drainage, telecom and street lamp mingle through the roof of the tunnel, particularly the gas pipe which is only several centimeters from the excavation surface. The cast iron gas pipe is much more sensitive to the settlement and deformation of the tunnel;

4) The exploration data indicates that the underground water here is abundant with a high water level. On one side large amount of water in the existing pipes might leak during the construction process which may bring hidden danger. On the other side, the excavation will result in the descending of the water level, so as the saltation clay consolidated and deformation weaken. This is especially unfavorable to the control of tunnel settlement and deformation;

5) The site is located at the heartland of Hefei of complex surrounding environment with large scale of cars and pedestrians. Dynamic load when cars passing through would leave grievous influence to the excavation which requires higher supporting demand.

3. NUMERICAL SIMULATION CALCULATION MODEL BUILDING**3.1. Calculation Parameters**

The surrounding rock classification belongs to V class. The primary lining is C25 concrete and the secondary lining is C30 reinforced concrete. All soil mechanical parameters are accessed on the basis of laboratory experiment and related standard, as shown in Table 1.

3.2. Finite Element Model

The least buried depth of this tunnel is about 2.5 m and the deepest 3.5 m. Tunnels of such depth belong to super shallow class. Although the underground water situation is complex, but when think over the sewerage, the unfavorable influence of the water towards the structure would not be taken into consideration.

The tunnel's supporting structure adopts the technology of composite lining of which twice support would be operated after excavation. The primary support is composed of section steel arch, mesh reinforcement and shotcrete. After the primary support reaches stable, the second lining will take off. The second lining is practiced by molded concrete. Therefore the pressure can be shared by both the primary support and the secondary lining. On the basis of the symmetry principle, when hand with underpass tunnel, only half need to be taken as the research object. Fig. (2) refers to the finite element model after elements dividing.

Table 1. Main physical and mechanical parameters.

Surrounding Rock Classification	Unit Weight (kN/m ³)	Deformation Modulus (GPa)	Poisson's Ratio	Internal Friction Angle (°)	Cohesive Force (MPa)
V	18	1.25	0.4	20	0.02

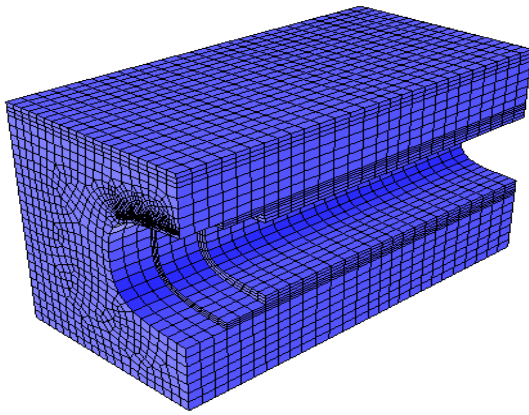


Fig. (2). Three-dimensional finite element calculation model.

4. CALCULATION RESULTS AND ANALYSIS

4.1. Construction Process and Load Step Setting

The entire length of the underground excavation part is 42 m among which 20 m pass through the road and 22 m under the plaza. In order to reflect the influence of the construction process to the structural internal force and deformation, all unite element calculation load step setting corresponds to the construction process. There are 9 load steps in total of this project while separately simulate the structural response of the construction process of underground excavation and lining during different period of the process. Table 2 refers to the process of the first 20 meters of the tunnel and the inside and outside lining.

4.2. Analysis of Displacement Dynamic Response

Fig. (3) refers to displacement time curve when the pavement is at the medial axis endpoint of the tunnel entrance. The data show that with the tunnel excavation proceeding on, obvious vertical displacement is generated at the vault. When the secondary load step surrounding rock starts excavating, displacement generates sharply. When operation of the third load step takes off, the change of the curve is found to weaken and becomes more flat after the 4th and the 5th load steps lining. This phenomenon indicates that after the excavation of the surrounding rock, compensation of stiffness in time could reduce the vault settlement. But since out lining stiffness is limited, the vault displacement still cannot be avoided completely. Besides the excavation and out lining of the 6th and 7th load steps, the inner lining also starts constructing. After the 7th load step's

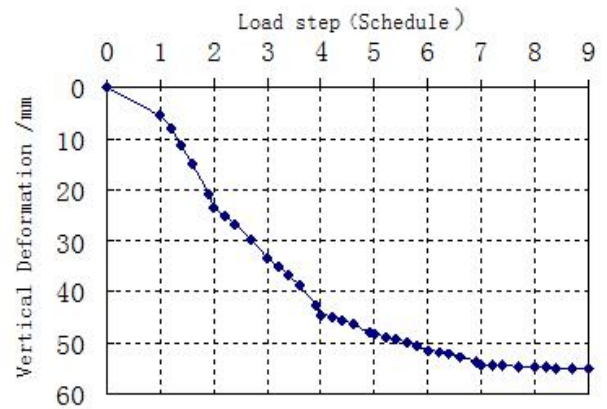


Fig. (3). Time history curves of displacement.

accomplishment the inner lining has achieved 10 m and the vault finally stabilized. This instructs that after the launch of load step surrounding rock's excavating as long as enough stiffness is compensated in time, the formation and deterioration of the displacement could be inhibited completely. The timely construction of the inner lining is proved to be the most efficient way on reducing displacement.

4.3 Analysis on Internal Force Response

Since the displacement of the vault is uneven after excavation, under the impact of both cover load and self-weight load of the pavement structure, significant flexural stress is generated. The stress is strong near the entrance of the tunnel and weak away from the entrance. This corresponds with the law of pavement deflection presentation and further illustrates that due to the lack of in time lining construction, the vault displacement caused by tunnel excavation will directly result in the generation of additional flexural stress of the pavement structure.

Fig. (4) represents the flexural stress time curve of the tunnel entrance medial axis endpoint. When the surrounding rock starts excavating, the flexural stress of the pavement structure corresponding to the entrance position increased rapidly. Stress curve becomes relatively flat, comparing the situation of no lining with the proceeding of the outer lining construction of the third load step. With further construction of the fourth and fifth load steps, the increasing rate of the flexural stress drops. This indicates that with the outer lining construction compensating the stiffness deficiency caused by the surrounding rock excavation, the following excavation

Table 2. Progress of excavation and inside and outside lining.

Excavation progress	Upper Bench	0	4	6	6.5	8.5	9.2	9.5	12	13	14	16	19	23.5
	Lower Bench	0	0	0	4	4	4	6	8	9	10	12	15	20.6
Primary Support	Upper Bench	0	4	6	6.5	8.5	9.2	9.5	12	13	14	16	19	23.5
	Lower Bench	0	0	0	4	4	4	6	8	9	10	12	15	20.6
The first lining		0	0	0	4	4	4	6	8	9	10	12	15	20.6
Secondary lining		0	0	0	0	0	0	0	6	6	6	10.8	10.8	10.8

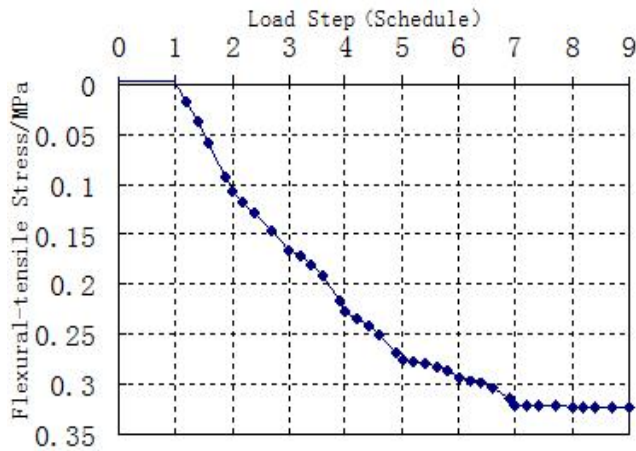


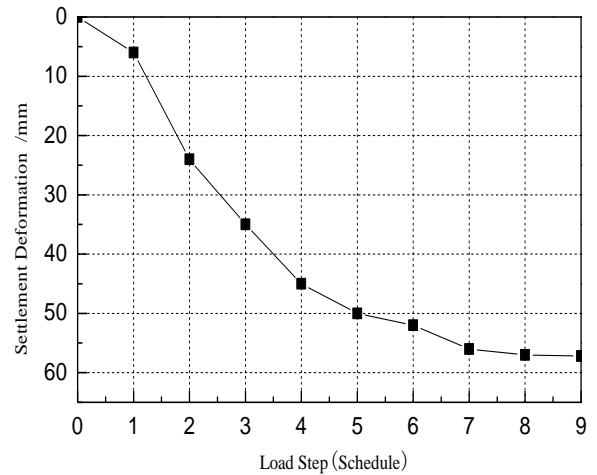
Fig. (4). Time history curves of flexural-tensile stress.

influences less to the pavement structure flexural stress. After the construction of the sixth load step inner lining, flexural stress increasing rate becomes more flat. And after the seventh load step, the inner lining reaches to 10 m and the pavement structure flexural stress completely stabilizes indicating that the follow-up construction leaves no influence to the pavement structure flexural stress. This perfectly corresponds to the result of the pavement structure influence caused by the tunnel excavation process reflected by the flexural stress time curve of the tunnel entrance medial axis endpoint.

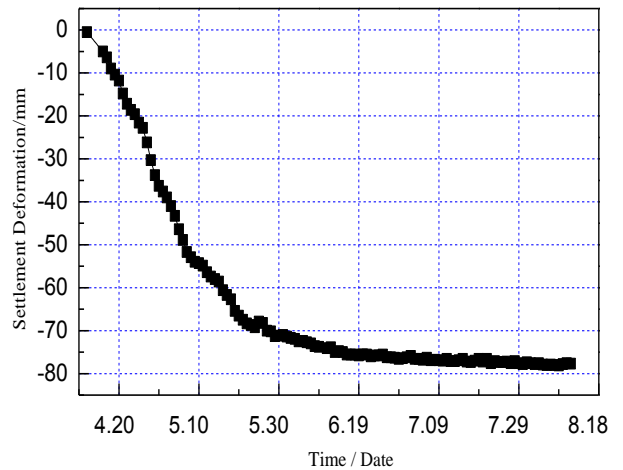
5. COMPARISON ANALYSIS OF THE SIMULATION CALCULATION AND MEASUREMENT RESULTS

Fig. (5a) refers to the curve of maximum settlement deformation at the cross section point with the load steps developing. The data show that obvious settlement and deformation are conducted along with the tunnel excavation. The deformation rate slightly slows down after the third load step's primary lining. The pavement settlement and deformation rate generally slow down when the secondary lining (the seventh load step) is finished. Fig. (5b) refers to the time curve of the measured settlement and deformation of that monitoring point. It can be concluded from this figure that when the tunnel excavation surface reaches the monitoring surface, the settlement curve declines precipitously. After the secondary lining of the monitoring point on May 4th, the settlement curve represents relatively obviously relax while the settlement remains increasing. This is on the contrary to the figures calculation in Fig. (5a) of which the reason might be some gaps are among the excavation face soil mass, primary lining and the secondary lining. Continuous settlement is conducted for the persistent compaction of the gaps.

Fig. (5a) indicates that the maximum surface settlement from the calculation is 5.7 cm while that from the measurement is 8cm. Since the water level tunnel layer is relatively high, while during the tunnel excavation, the level declines and therefore resulted in the water loss of the excavation face soil mass. On one hand the water level decline increased the effective stress of the soil mass and deformation occurred, on the other hand serious shrinkage



(a) Results of finite element calculation



(b) Results of measurement

Fig. (5). Land subsidence comparison diagrams of finite element calculation and measurement.

deformation was generated during the water loss of the saturated silt clay. In the 3D numerical analysis, the influence of the underground water towards surface settlement was left out of consideration, so the predicated surface settlement was appreciably less than the measured.

Fig. (6) refers to the surface cross section settlement curve of different positions to the tunnel entrance after the 6th load step is finished (secondary lining of the 6-m accelerator section). As shown in the graph, the deformation near the entrance is more severe. The settlement curve becomes more flat with the distance increase. Fig. (6b) refers to the different monitoring cross section settlement curve of the secondary lining before the 6-meter is finished. The law of the measured settlement curve coincides to the calculated value.

Through the comparison between Figs. (6 and 7), the predicted maximum surface settlement and law through large-scale finite element calculation software of ABAQUS are almost the same with the measured value. This indicates that 3D dynamic numerical simulation could objectively

reflect the genuine situation of the tunnel excavation afterwards have better influence on guiding and optimizing the tunnel construction.

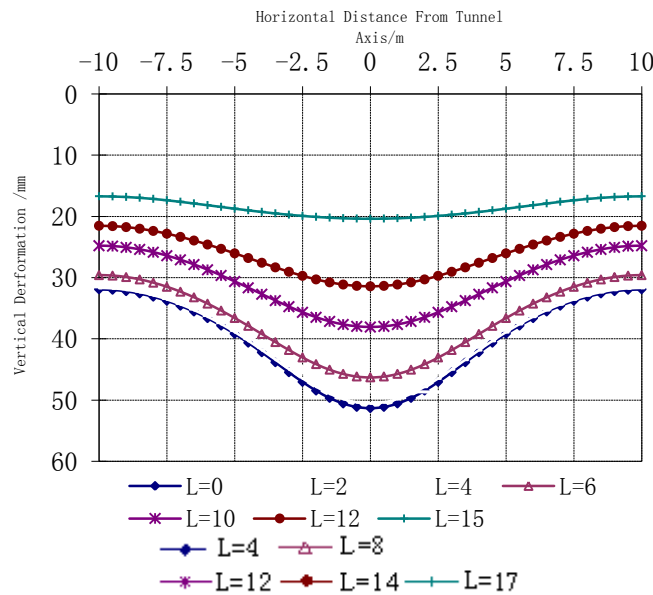
Fig. (6) refers to the surface cross section settlement curve of different positions to the tunnel entrance after the 6th load step is finished (secondary lining of the 6-meter accelerator section). As shown in the graph, the deformation near the entrance is more severe. The settlement curve becomes more flat with the distance increase. Fig. (6b) refers to the different monitoring cross section settlement curve of the secondary lining before the 6-m is finished. The law of the measured settlement curve coincides to the calculated value.

Through the comparison between Figs. (6 and 7), the predicted maximum surface settlement and law through large-scale finite element calculation software of ABAQUS

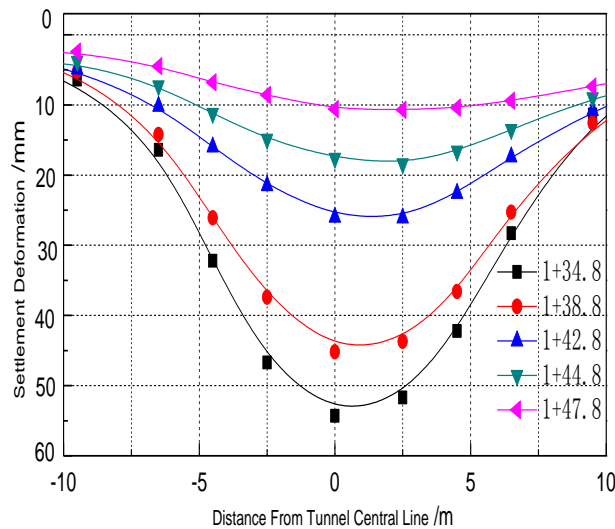
are almost the same with the measured value. This indicates that 3D dynamic numerical simulation could objectively reflect the genuine situation of the tunnel excavation afterwards have better influence on guiding and optimizing the tunnel construction.

CONCLUSION

- (1) It can be seen from the construction of city plaza underground tunnel that under complex geological situation, the combined technology of long pipe roof and small duct pregrouting construction techniques is feasible. Undermining method can avoid the traffic congestion brought by open cut and underground pipes migration in complex situation, failure of ensuring limit time and serious problems. This is proved to be the best scheme of city construction.



(a) Results of finite element calculation



(b) Results of measurement

Fig. (6). Cross section settlement comparison diagrams of finite element calculation and measurement.

(2) Taking factors like time-space effect, excavation sequence, support form into consideration, utilizing finite element calculation software of ABAQUS to do the analysis on the displacement and stress dynamic response during tunnel excavation process. And through the comparison analysis between the simulation calculation and the field measurement value, data simulation is turned out to reflect the law of surface settlement during tunnel constructing objectively, and meanwhile ensure the safety of buildings around.

CONFLICT OF INTEREST

The authors confirm that this article content has no conflict of interest.

ACKNOWLEDGEMENTS

The paper is funded by the Natural Science Foundation of Anhui Province, China (1308085QE85), and funding project of HeFei rail transit Construction Safety Supervision Station (2014CGFZ0199).

REFERENCES

- [1] Q. Qihu, "Modern technology of underground space development and utilization in city and its developing trend", *Railway construction technology*, vol.5, pp.1-6, 2000.
- [2] Q. Qihu, "Sustainable development of the cities and the development and utilization of underground space", *Underground Space*, vol.18, pp. 69-74, Feb 1998.
- [3] T. Lin-xu, "Underground space and future city", *Chinese Journal of Underground Space and Engineering*, vol.1, pp. 323-328, Mar 2005.
- [4] Z. Xiao-wen, and P. Jia-liu, "Centrifuge model test on ground settlement induced by tunneling in sandy soil", *Rock and Soil Mechanics*, vol. 23, pp. 559-563, May 2002.
- [5] W. Gang, "Prediction on ground deformation induced by shield tunneling construction", *Chinese Journal of Rock Mechanics and Engineering*, vol. 28, pp. 418-424, Feb 2009.
- [6] C. Liang, H. Hongwei, and Wang Rulu, "Analysis of the observed longitudinal settlement of a tunnel caused by an adjacent shield tunneling on top", *China Civil Engineering Journal*, vol.39, pp. 84~87, Jun 2002.
- [7] W. Meng-shu, *Technology of Shallow Tunnel Excavation*, Hefei: Anhui Education Press, 2004.
- [8] Z. Zhi-guo, H. Mao-song, and W. Wei-dong, "Analysis on response of existing tunnels due to adjacent tunneling in multi-layered soils", *Chinese Journal of Geotechnical Engineering*, vol.31, pp. 600-608, Apr 2009.

Received: April 02, 2014

Revised: July 16, 2014

Accepted: July 16, 2014

© Wang et al.; Licensee *Bentham Open*.

This is an open access article licensed under the terms of the Creative Commons Attribution Non-Commercial License (<http://creativecommons.org/licenses/by-nc/3.0/>) which permits unrestricted, non-commercial use, distribution and reproduction in any medium, provided the work is properly cited.